

Theory of Charge Order and Heavy-Electron Formation in the Mixed-Valence Compound KNi_2Se_2

James M. Murray and Zlatko Tešanović

*Institute for Quantum Matter and Department of Physics and Astronomy,
Johns Hopkins University, Baltimore, MD 21218*

(Dated: May 16, 2022)

The material KNi_2Se_2 has recently been shown to possess a number of striking physical properties, many of which are apparently related to the mixed valency of this system, in which there is on average one quasi-localized electron per every two Ni sites. Remarkably, the material exhibits a charge density wave (CDW) phase that disappears upon cooling, giving way to a low-temperature coherent phase characterized by an enhanced electron mass, reduced resistivity, and an enlarged unit cell free of structural distortion. Starting from an extended periodic Anderson model and using the slave-boson formulation, we develop a model for this system and study its properties within mean-field theory. We find a reentrant first-order transition from a CDW phase, in which the localized moments form singlet dimers, to a heavy Fermi liquid phase as temperature is lowered. The magnetic susceptibility is Pauli-like in both the high- and low-temperature regions, illustrating the lack of a single-ion Kondo regime such as that usually found in heavy-fermion materials.

Heavy-fermion materials exhibit a host of fascinating collective quantum behaviors, which have made them a major focus of ongoing research for over three decades [1, 2]. The “standard model” of heavy-fermion behavior, as depicted in the famed Doniach diagram [3], features competition between the heavy Fermi liquid phase, stabilized by the hybridization between conduction electrons and localized moments, and a magnetic phase, typically stabilized by the RKKY interaction between the localized moments. An intriguing possibility that has received comparatively little attention is the existence of charge order, rather than the usual magnetic order, in proximity to the heavy-fermion state. Mixed-valency systems [4], which contain a variable number of localized electrons per atomic site, are a natural place to look for such competing effects. If the fractional filling takes a commensurate value, then Coulomb repulsion between electrons on nearby sites may induce charge density wave (CDW) ordering. Mixed valency has been studied recently in f -electron materials exhibiting heavy-fermion behavior [5–7], as well as in the context of the related “charge Kondo effect” [8, 9]. However, in both of those cases the emphasis has generally been on the single-site valency as hybridization or interaction between electrons is increased, rather than on the possibility of collective CDW formation and competition of this charge order with the heavy fermion phase.

The material KNi_2Se_2 has recently been shown to exhibit several remarkable physical properties [10], many of which appear to be related to its mixed-valent nature. At high temperatures the material has high resistivity; the magnetic susceptibility is constant, indicating Pauli paramagnetic response; and structural analysis reveals that the material has at least three distinct subpopulations of Ni-Ni bond lengths. Upon cooling below $T_{\text{coh}} \approx 20\text{K}$, the resistivity rapidly decreases, the structural distortions disappear, and the material enters a co-

herent heavy-fermion state with effective electron mass $m^* \sim 10m_0$, eventually giving way to superconductivity below $T_c \approx 1\text{K}$. This material is also unusual in that an applied magnetic field induces virtually no response in the measured specific heat and magnetoresistivity, indicating that the low-temperature coherent phase does not arise from competition with local magnetic order as in typical heavy-fermion materials. Rather, it was proposed that the coherent state competes with a *charge-fluctuating* state, facilitated by the mixed valency of the Ni ions in KNi_2Se_2 [10]. The proximity of this system to charge (rather than magnetic) order, the disappearance of the CDW as temperature is lowered, and the lack of common signatures of Kondo-like behavior in the magnetic response together distinguish this material from conventional heavy-electron systems, making it a new and fascinating example of the diversity of effects that can be observed in these materials.

In this study, we present a theory that captures the key ingredients that characterize this system. At high temperatures, the quasi-localized electrons in our model form a CDW and pair with one another into singlet dimers, which explains the observed structural distortion and insensitivity to applied magnetic field. As temperature is lowered, the CDW dissolves in a first-order transition directly into a spatially uniform, correlated heavy-fermion state, without the intermediate single-ion Kondo regime that is usually observed in heavy-fermion materials. The details of this model and the main results of the calculations are presented below.

KNi_2Se_2 has a quasi-two-dimensional, layered structure, with the Ni and Se ions alternating in checkerboard fashion on a square lattice within each layer. Consideration of the stoichiometry reveals that the effective valency of Ni in this compound is “1.5+,” so that at low energies the effective degree of freedom is one quasi-localized d -electron with spin $1/2$ per every two Ni sites, with a

small amplitude for these electrons to hop to neighboring Ni sites. Conduction electron bands are formed from the other Ni and Se orbitals and have a significantly greater bandwidth than the quasi-localized d -electrons.

With this picture in mind, the following Hamiltonian describing the “extended periodic Anderson model” provides a useful starting point:

$$\begin{aligned}
 H_{\text{EA}} = & -t_c \sum_{\langle ij \rangle} (c_{i\sigma}^\dagger c_{j\sigma} + H.c.) - t_f \sum_{\langle ij \rangle} (d_{i\sigma}^\dagger d_{j\sigma} + H.c.) \\
 & - \varepsilon_f \sum_i n_{di} + V \sum_i (d_{i\sigma}^\dagger c_{i\sigma} + H.c.) \\
 & + U \sum_i n_{d\uparrow} n_{d\downarrow} + \sum_{i \neq j} W_{ij} n_{di} n_{dj},
 \end{aligned} \quad (1)$$

where i, j denote Ni sites on a two-dimensional square lattice. The first term in this equation describes hopping of the conduction electrons. The second and third terms describe the hopping and on-site energy of quasi-localized electrons on neighboring Ni sites. The fourth term describes hybridization between the two types of electrons. Finally, the last two terms describe Coulomb repulsion of d -electrons occupying the same site and nearby sites, where $n_{di\sigma} = d_{i\sigma}^\dagger d_{i\sigma}$. Summation over repeated spin indices is implicit in (1). The Hamiltonian is identical to the well-known periodic Anderson model, with the addition of the W term describing intersite Coulomb repulsion. This term is typically neglected in describing heavy fermion materials due to the fact that such systems usually have exactly one local moment per site, so such a Coulomb term effectively adds an overall constant to the total energy. Such a term is crucial for a system such as KNi_2Se_2 near one quarter filling, however, since such systems are susceptible to Coulomb repulsion-driven charge ordering.

In the limit of large on-site repulsion U , it is convenient to enforce the constraint of no double occupancy through the introduction of slave boson operators [11–13]. In this formulation, we substitute $d_{i\sigma} = b_i^\dagger f_{i\sigma}$, where $f_{i\sigma}$ describes a charge-neutral “spinon” that carries the spin of the electron, and the slave boson operator b_i describes a spinless particle with positive charge. Within this formalism, rather than having to enforce the constraint $n_{di} \leq 1$ at every site, one instead has the constraint $n_{fi} + b_i^\dagger b_i = 1$, where $n_{fi} = f_{i\uparrow}^\dagger f_{i\uparrow} + f_{i\downarrow}^\dagger f_{i\downarrow}$ is the number operator for spinons. In terms of these new operators, the Hamiltonian (1) becomes

$$\begin{aligned}
 H = & H_c + H_{fc} + H_f + H_W + H_\lambda + H_J \quad (2) \\
 H_c = & -t_c \sum_{\langle ij \rangle} (c_{i\sigma}^\dagger c_{j\sigma} + H.c.) \\
 H_{fc} = & V \sum_i (b_i f_{i\sigma}^\dagger c_{i\sigma} + H.c.) \\
 H_f = & -t_f \sum_{\langle ij \rangle} (b_i b_j^\dagger f_{i\sigma}^\dagger f_{j\sigma} + H.c.) - \varepsilon_f \sum_i n_{fi}
 \end{aligned}$$

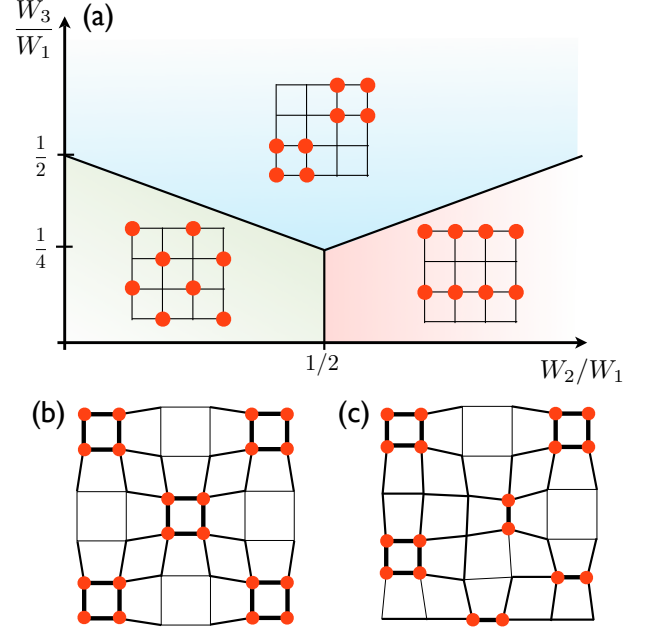


FIG. 1. (a) $T = 0$ diagram of CDW phases for various values of second- and third-neighbor Coulomb repulsion, with $J = V = 0$. (b) Schematic illustration of the “plaquette” phase showing expected lattice distortion once the coupling between electron and lattice degrees of freedom is taken into account. Links connecting sites containing localized electrons are shorter and are represented by thicker lines. (c) Schematic illustration of a possible configuration in the case where long-range CDW order is absent, but the singlet nature of the state and distribution of bond lengths remain similar to those shown in (b).

$$\begin{aligned}
 H_W = & \sum_{i \neq j} W_{ij} n_{fi} n_{fj} \\
 H_\lambda = & i \sum_i \lambda_i (n_{fi} + b_i^\dagger b_i - 1) \\
 H_J = & J \sum_{\langle ij \rangle} \mathbf{S}_i \cdot \mathbf{S}_j
 \end{aligned}$$

The first four terms in (2) are analogous to terms appearing in (1), but rewritten in the slave boson description. H_λ replaces the on-site repulsion term in (1) by enforcing the constraint of no double occupancy for spinons via the Lagrange multiplier field λ_i . The last term in (2) describes an antiferromagnetic Heisenberg interaction driven by superexchange between spins on neighboring sites. The Hamiltonian (2) is identical to the “Anderson–Heisenberg” model that has been studied recently [14–16], with the addition of the Coulomb term H_W .

Figure 1(a) shows the phase diagram with the possible CDW phases for various values of first-, second-, and third-nearest neighbor repulsion (W_1 , W_2 , and W_3 , respectively). We choose parameters such that the “plaquette” CDW phase in the upper part of Figure 1(a) is realized, since this phase naturally allows for dimer

formation between neighboring spinons. Note that, due to the frustration between the competing tendencies for large W_1 and W_2 , the realization of this phase does not require especially large values of third-neighbor repulsion W_3 . For example, the plaquette CDW phase is realized in the idealized case of unscreened $\sim 1/r$ Coulomb repulsion, for which the ratios of the repulsion terms are $W_2/W_1 = 1/\sqrt{2}$ and $W_3/W_1 = 1/2$. When coupling between electronic and lattice degrees of freedom is taken into account, such a picture can also explain the distinct peaks in the distribution of bond lengths observed at $T > T_{\text{coh}}$ via neutron pair distribution function analysis [10], since links containing a singlet pair can be expected to be shorter than other links. It can be seen from Figure 1(b) that each unit cell contains 2 short bonds, 2 long bonds, and 4 bonds of medium length. This is consistent with the three peaks in the distribution of bond lengths observed in experiment, with the central peak larger than the others. While there is no clear experimental evidence of long-range spatial order such as that described here, we expect that the key features of this model—spatially modulated electron density and singlet formation at high temperatures, giving way to a spatially uniform coherent state at low temperatures—will remain valid even in the absence of long-range order, as illustrated schematically in Figure 1(c).

We proceed to study the Hamiltonian (2) within mean-field theory. Denoting as sublattice A (B) the sites shown as (un)occupied in the figure, the average occupation number is taken to be $\langle n_{fi} \rangle = n_f + \zeta_i \frac{\Delta}{2}$, where n_f is the average density of spinons per site, Δ is the CDW order parameter, and $\zeta_i = \pm 1$ on sublattice A (B). At mean-field level, the nearest neighbor and second neighbor Coulomb terms $W_{1,2}$ merely shift the chemical potential for the spinons, so they will not be considered further here. The Lagrange multiplier field λ_i and the slave boson field b_i are also treated as staggered mean fields: $i\lambda_i = \lambda_0 + \zeta_i \lambda_1$ and $b_i = b_0 - \zeta_i b_1$, with $\lambda_{0,1}$ and $b_{0,1}$ real. The Heisenberg spins \mathbf{S}_i are expressed in terms of spinons: $S_i^a = \frac{1}{2} f_{i\alpha}^\dagger \sigma_{\alpha\beta}^a f_{i\beta}$, where σ^a are the Pauli matrices. Defining the mean fields $\chi_{A,A',B,AB} = \langle f_{i\sigma}^\dagger f_{j\sigma} \rangle$, with χ_{AB} defined on links between sites on different sublattices, χ_B on links between two sites on sublattice B, and $\chi_{A(A')}$ on links between two sites on sublattice A in the $x(y)$ -direction. It is found that the free energy is always lowered in the CDW phase by having only one of $\chi_A, \chi_{A'}$ nonzero, so that the four spins on each plaquette form two dimers. In the uniform phase, χ_{ij} takes the same value on all links.

In solving the mean-field equations, we require that the density of spinons is fixed to $n_f = 0.5$ spinons per site in the limit $V = 0$, which is accomplished by appropriately setting the on-site energy of the spinons ε_f . Once the hybridization V is nonzero, ε_f remains fixed to this value, and in general $n_f \neq 0.5$ once V is finite.

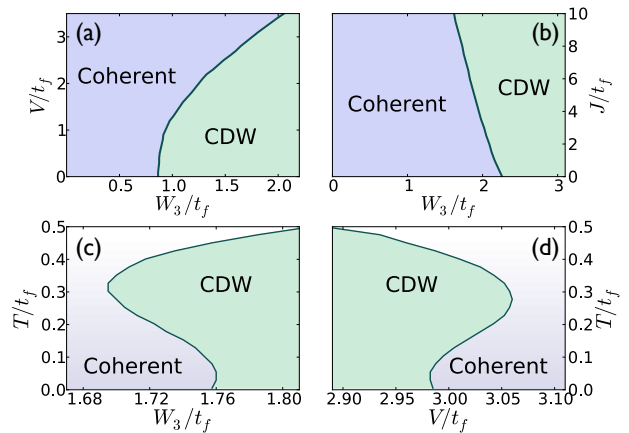


FIG. 2. Upper plots show the $T = 0$ phase diagrams for V vs. W_3 with $J = 8t_f$ (a), and for J vs. W_3 with $V = 3t_f$ (b). Lower plots show the reentrant first-order transition to the charge-ordered phase as a function of W_3 with $V = 3t_f$ (c), and as a function of V with $W_3 = 1.75t_f$ (d), and with $J = 8t_f$ in both plots.

The chemical potential is set to keep the total density of particles in the system fixed at $n_c + n_f = 1.3$ per site, which remains fixed even for $V \neq 0$. The results that follow are not particularly sensitive to the choice of n_c , so long as $n_c > n_f$, so that there are enough conduction electrons to screen all of the local moments in the coherent phase. The ratio of hopping amplitudes for spinons and c -electrons has been set to $t_f/t_c = 0.2$, which is substantially larger than that found in typical heavy-fermion systems. This is a reflection of the fact that the localized moments in KNi_2Se_2 are d -electrons, which are less tightly bound to their atomic cores than the f -electrons that constitute the local moments in most other heavy-fermion systems. This relatively small ratio of bandwidths is also the reason for the rather modest effective mass enhancement of $m^* \sim 10m_0$ [10], which is $10 \sim 100$ times smaller than that typically found in f -electron heavy fermions.

The phase diagrams shown in Figure 2 illustrate the existence of a reentrant, first-order transition from a CDW to a spatially uniform phase upon cooling. This behavior is rather unusual, as in most systems the phase that breaks translational symmetry is the ground state that is realized as $T \rightarrow 0$. While the reentrance occurs along the entire critical line in Figure 2(a), it emerges along the critical line in Figure 2(b) only for $J \gtrsim 3t_f$, growing in extent as J is increased. These values of J are rather large to be generated by superexchange alone, for which one expects $J \sim t_f^2/U$. It has been suggested that additional contributions might arise in similar contexts from other superexchange processes in the CDW phase [17], or from RKKY interactions at low temperatures [16, 18]. Reentrant behavior reminiscent of that shown here has been seen previously in a theory of simple checkerboard

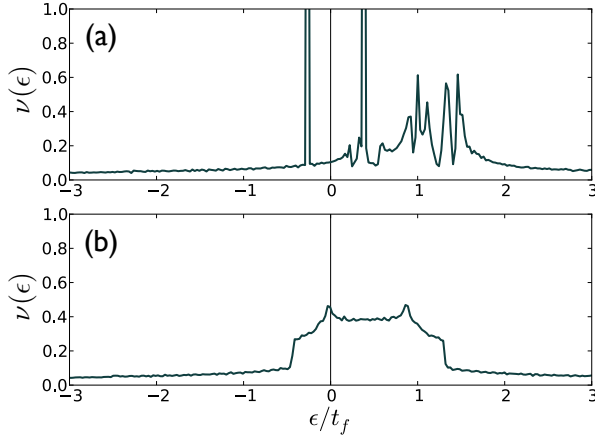


FIG. 3. Densities of states for the CDW phase at $T = 0.15t_f$ (a) and the coherent phase at $T = 0.01t_f$ (b), with $W_3 = 1.75t_f$, $J = 8t_f$ and $V = 3t_f$. The Fermi level is at $\epsilon = 0$.

CDW ordering at $1/4$ filling in layered molecular crystals [19], although in that case only a second-order transition was found. The model presented here also exhibits a second-order transition, but only at higher temperatures than those shown in Figure 2. The mean field χ_A is nonzero throughout the CDW phase shown in Figure 2, up to $T \sim 0.6t_f$, indicating that singlet formation is taking place between the localized spinons.

For the parameters given above, there is a jump in the average spinon occupation per site n_f at the first-order transition. At $W_3 = 1.75t_f$, the occupation jumps from $n_f = 0.45$ for $T < T_{\text{coh}} = 0.12t_f$ to $n_f = 0.53$ for $T > T_{\text{coh}}$. The reduced valency $n_f < 0.5$ in the uniform phase is expected, indicating that some of the spinons become delocalized and join the sea of conduction electrons in forming a heavy Fermi liquid. The increased valency in the CDW phase is less expected, but is consistent with the lack of long-range CDW order observed in experiment [10], since a long-range ordered state would be impossible at incommensurate filling. The valency of localized electrons, which is given by n_f on account of the constraint $\langle n_{fi} \rangle + b_i^2 = 1$, can be measured using techniques such as resonant inelastic X-ray scattering [20]. It would be interesting to test whether the predicted jump in n_f at $T = T_{\text{coh}}$ could be observed experimentally.

The densities of states in the two phases are shown in Figure 3. In the CDW phase, the well-defined peaks above and below the Fermi level clearly show that the spinon excitations are gapped. In contrast, the spinons contribute to the hybridization peak at the Fermi level in the low-temperature phase, as is typical in heavy-fermion materials. The relative magnitude of the peak in this case, however, is substantially smaller than that in f -electron materials. Comparing the values of the densities of states at the Fermi level in the two different phases, one finds an enhancement of ≈ 3.0 in the normal phase rela-

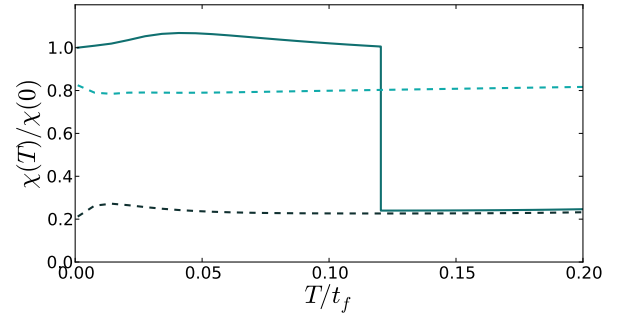


FIG. 4. Uniform magnetic susceptibility with $W_3 = 1.75t_f$ and $J = 8t_f$. The light and dark dashed lines show $\chi(T)$ in the uniform phase ($V = 4t_f$) and in the CDW phase ($V = 2t_f$), respectively. The solid line shows $\chi(T)$ for $V = 3t_f$, which exhibits a phase transition at $T = T_{\text{coh}} = 0.12t_f$. All plots are normalized to $\chi(0)$ for the solid curve.

tive to the CDW phase. This can be compared with measurements on KNi_2Se_2 , where an enhancement of ≈ 3.1 was observed in the electronic specific heat coefficient γ for $T < T_{\text{coh}}$ [10].

The uniform magnetic susceptibility can be calculated as the derivative of magnetization with respect to applied magnetic field. Figure 4 shows the susceptibility as a function of temperature, assuming that the Lande g -factors for conduction electrons and spinons are equal. The approximately constant susceptibility in the region $T < 0.12t_f = T_{\text{coh}}$ corresponds to the Pauli susceptibility of the heavy Fermi liquid, in which the conduction electrons are hybridized with the localized spinons, leading to an enhanced density of states near the Fermi level. At T_{coh} , there is a jump in the susceptibility to a much smaller constant value, indicating that only the conduction electrons contribute to the susceptibility at $T > T_{\text{coh}}$, while the spinons form singlet pairs. This is in contrast to the Curie susceptibility $\chi \sim 1/T$ that is typically observed at high temperatures in heavy-fermion materials.

Rather than exhibiting a sharp step, however, the experimentally measured $\chi(T)$ remains approximately constant through the CDW transition [10]. One possible explanation for this discrepancy is the Van Vleck contribution to $\chi(T)$, which has not been included in our model. The possibility of a large contribution of this type in heavy-fermion materials has been considered previously [21]. Others have since investigated the Van Vleck contribution to the susceptibility and have found that, when multiple localized bands are approximately degenerate, one generally has $\chi_V \sim \chi_{\text{Pauli}}$ [22–24]. Thus if an unhybridized band that was not included in our model has large spectral weight near one of the peaks in Figure 3(a), an increased χ_V could compensate for the decrease in χ_{Pauli} at higher temperatures, with the sum of the two terms remaining roughly constant. Calculating the pre-

cise Van Vleck contribution to the susceptibility would require a more detailed knowledge of the band structure, however, and so we leave this as an open question to be addressed in future work.

In conclusion, we have provided a theoretical framework for describing the key properties of the recently discovered mixed-valency material KNi_2Se_2 , most importantly the vanishing of the CDW phase upon cooling. The formation of singlet dimers by the local moments in the CDW phase explains the lack of common signatures of single-ion Kondo behavior, such as a Curie susceptibility at high temperatures. This mechanism may also explain the lack of a resistivity peak in measurements on KNi_2Se_2 [10]. Such a peak typically forms in heavy-fermion materials at temperatures just above the coherence temperature, where the Kondo screening clouds act as spin-flip scattering centers but are not yet coherent with one another. A direct transition from a singlet CDW phase to a coherent low-temperature phase precludes this possibility, however, and is consistent with the monotonically decreasing resistivity observed in experiment as T is lowered. This material illustrates the potential of mixed-valency systems for exhibiting a rich array of collective quantum behaviors.

We thank J. Kang, T. McQueen, J. Neilson, O. Tchernyshyov, and Y. Wan for helpful discussions. This work was supported by the Johns Hopkins–Princeton Institute for Quantum Matter, under Grant No. DE-FG02-08ER46544 from the US Department of Energy, Office of Basic Energy Sciences, Division of Materials Sciences and Engineering.

-
- [1] P. Coleman, in *Handbook of Magnetism and Advanced Magnetic Materials*, edited by H. Kronmüller and S. Parkin (Wiley, New York, 2007), p. 95–148.
 - [2] A. C. Hewson, *The Kondo Problem to Heavy Fermions* (Cambridge Univ. Press, Cambridge, 1993).
 - [3] S. Doniach, *Physica B* **91**, 231 (1977).
 - [4] C. Varma, *Rev. Mod. Phys.* **48**, 219 (1976).
 - [5] K. Kummer *et al.*, *Phys. Rev. B* **84**, 245114 (2011).
 - [6] A. Fernandez-Pañella, *et al.*, *Phys. Rev. B* **86**, 125104 (2012).
 - [7] S. Watanabe and K. Miyake, *J. Phys. Cond. Mat.* **23**, 094217 (2011).
 - [8] A. Taraphder and P. Coleman, *Phys. Rev. Lett.* **66**, 2814 (1991).
 - [9] H. Matsuura and K. Miyake, arXiv:1209.5519 (2012).
 - [10] J. R. Neilson *et al.*, *Phys. Rev. B* **86**, 054512 (2012).
 - [11] N. Read and D. M. Newns, *J. Phys. C* **16**, 3237 (1983).
 - [12] P. Coleman, *Phys. Rev. B* **29**, 3035 (1984).
 - [13] D. M. Newns and N. Read, *Adv. Phys.* **36**, 799 (1987).
 - [14] C. Pepin, *Phys. Rev. Lett.* **98**, 206401 (2007).
 - [15] J.-X. Zhu, I. Martin, and A. R. Bishop, *Phys. Rev. Lett.* **100**, 236403 (2008).
 - [16] M.-T. Tran, *Phys. Rev. B* **85**, 165118 (2012).
 - [17] R. H. McKenzie *et al.*, *Phys. Rev. B* **64**, 085109 (2001).
 - [18] P. Coleman and N. Andrei, *J. Phys. Cond. Mat.* **1**, 4057 (1989).
 - [19] J. Merino and R. H. McKenzie, *Phys. Rev. Lett.* **87**, 237002 (2001).
 - [20] C. Dallera *et al.*, *Phys. Rev. Lett.* **88**, 196403 (2002).
 - [21] Z. Zou and P. W. Anderson, *Phys. Rev. Lett.* **57**, 2073 (1986); F. C. Zhang and T. K. Lee, *ibid* **58**, 2728 (1987); G. Aeppli and C. M. Varma, *ibid* **58**, 2729 (1987); D. L. Cox, *ibid* **58**, 2730 (1987).
 - [22] S. M. M. Evans, *J. Phys. Cond. Mat.* **2**, 9097 (1990).
 - [23] H. Kontani and K. Yamada, *J. Phys. Soc. Japan* **65**, 172 (1996).
 - [24] T. Mutou and D. S. Hirashima, *J. Phys. Soc. Japan* **65**, 369 (1996).